DOI: 10.13009/EUCASS2017-317

GNC architecture for the e.Deorbit mission

*Jürgen Telaar, Ingo Ahrns, Stéphane Estable**
*Wolfgang Rackl, Marco De Stefano, Roberto Lampariello***
*Nuno Santos, Pedro Serra, Marco Canetri****
*Finn Ankersen, Jesus Gil-Fernandez*****
**Airbus Defence and Space*
Airbus-Allee 1, 28199 Bremen, Germany
***Institute of Robotics and Mechatronics, DLR*
Münchner Str. 20, 82234 Wessling, Germany
**** GMV*
Av. D. João II, Lote 1.17.02 - Torre Fernão de Magalhães, 7, 1998-025 Lisbon, Portugal
*****ESA*
Keplerlaan 1, 2201 AZ Noordwijk, Netherlands

Abstract
The GNC architecture presented in this paper has been developed in the frame of e.Deorbit phase B1. The architecture is dedicated to approach and capture the uncooperative target satellite Envisat, comprising ascent from launch orbit to the target orbit, rendezvous with the target satellite, capture and stabilisation of the coupled system and de-orbiting.
The homing and closing trajectories are based on e/i separation allowing a passively safe approach until the proximity operations begin. The chaser has to synchronise its motion with the target due to its large dimensions. The safety monitoring concept is briefly discussed.
The propellant budget and the GNC performance requirements are consolidated by Monte Carlo simulations.

1. Introduction

Envisat is a former Earth remote sensing satellite which contributed for 10 years to climate monitoring and research. With about 8 tons launch mass it was ESA's largest Earth observation satellite. Due to its high mass and collision probability with other satellites in sun-synchronous orbits Envisat is on top of the list of space debris objects which need to be removed urgently in order to avoid the Kessler syndrome [1].
The e.Deorbit program is devoted to remove Envisat safely from orbit. The system design is mainly driven by the propellant consumption required for ascent and phasing from launch injection orbit to the target orbit, rendezvous and capture, and for the de-orbiting manoeuvre. The GNC architecture for this challenging mission is based on a navigation sensor suite allowing relative navigation from far range (8 km) until proximity operations and capture. The capture system is a robot arm equipped with a stereo camera and an illumination unit. The gripper is designed for grasping Envisat's launch adapter ring. Due to the limited length of the robot arm and due to Envisat's dimensions, the chaser needs an actuator system which allows tracking the tumbling motion of the target. The inherent collision risk during the capture manoeuvre requires an efficient and reactive safety monitoring concept.

2. e.Deorbit Mission Overview

Figure 1 gives an overview about the mission phases depending on the distance between chaser and target, and shows which sensors are active during the rendezvous phase. The Chaser satellite is launched into a low earth orbit and performs the ascent and phasing towards the Target employing its main engines. These manoeuvres are based on absolute navigation, meaning that the Target orbit is determined from ground by radar measurements while the Chaser orbit is estimated based on GPS (global positioning system) measurements. The Chaser receives ΔV commands from ground for the ascent and phasing. At the Rendezvous Entry Gate the distance between Chaser and Target is within the range of the relative navigation sensors, the Target is identified and the relative navigation starts. The Rendezvous Entry Gate and the approach until Save Hold Point are based on e/i-separation, meaning that the

DOI: 10.13009/EUCASS2017-317

orbits of Chaser and Target have no point of intersection and are therefore passively safe. The natural motion of the Chaser relative to the Target can be described by an ellipse, if the semi-major axes of the two satellite orbits are the same. This ellipse is defined by a radial component (in the orbit plane) and a cross track component. The radial and the along track motion are coupled. The along track dimension of this ellipse is twice as large as the radial component. The centre of this ellipse can be positioned as needed for the mission, e.g. 8 km behind the target for the Rendezvous Entry Gate. For more explanations regarding e/i-separation and the trajectory planning based on Relative Orbital Elements (ROE) refer to [2] and [3].

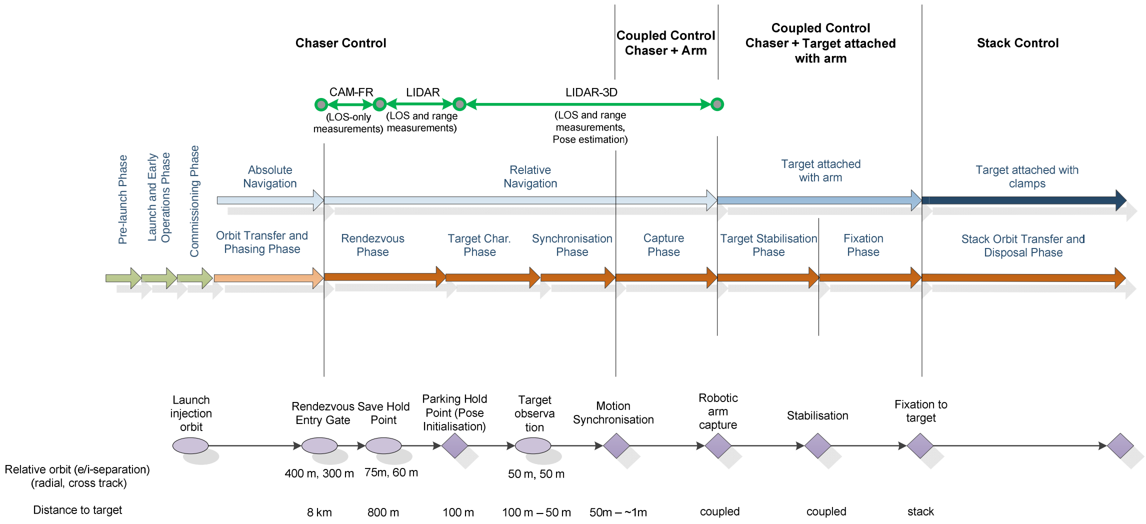

Figure 1 e.Deorbit mission phases

In the beginning of the rendezvous phase only line of sight measurements provided by a narrow angle camera (CAM-N) are available. As soon as the distance drops below approximately 1 km, the Target is within the range of the scanning LIDAR (Light Detection And Ranging), which measures the line of sight and the range. At the Parking Hold Point, about 100 m behind the Target on the V-bar, the LIDAR is switched to LIDAR-3D mode allowing full pose estimation, i.e. relative position and attitude are determined by image processing of the detected point cloud of the scanning LIDAR. The image processing significantly improves the relative position measurement performance compared to the simple centroiding algorithm of the LIDAR. At the Parking Hold Point first detailed images of the Target are taken. Then a fly-around is performed to gather more information about the Target structural integrity and shape. If the shape of the target differs significantly from the model used for the pose estimation, the model will be updated based on the data gathered in the Target characterisation phase.
The proximity operations start with the approach along the V-bar to 30 m distance to the target. Next a fly-around to the Target's angular momentum vector is performed. The Chaser further approaches the Target along its angular momentum vector and synchronises its motion with the Target. The motion of the Chaser is controlled relatively to the grasping point at the launch adapter ring of the Target. Due to Envisat's tumbling motion the Chaser has to follow a trajectory which is determined by the angular rate and by the moments of inertia of the Target. The Chaser has basically to compensate the centrifugal forces along this trajectory and the forces and torques from the robot arm acting at the arm base.
While the Chaser performs station keeping relatively to this point, the robot arm moves the gripper to the grasping point at the launch adapter ring. An illumination unit and a camera system mounted close to the gripper support this manoeuvre. The illumination unit is necessary to cover phases during which the grasping point is shadowed by the Chaser or the Target itself. The contact forces between end-effector and Target shall be limited in order to avoid significant transfer of energy and impulse to the Target as well as bouncing off after first contact. Therefore the positioning of the end-effector is performed in impedance control mode. The impedance control mode allows the robot to react to impacts with the environment with a predefined behaviour, practically complying with the impact force like a soft spring. The stiffness of the control during grasping can be defined independently for each of the six degrees of freedom. This feature allows for example controlling the axis of approach direction softly to avoid exchange of energy and impulse, while the other axes are controlled stiffer to precisely position the gripper.
After successful grasping, the robot arm is rigidised, meaning that the angular rates in the joints are reduced until their brakes can be engaged. Then the coupled system of Chaser and Target is stabilised using the attitude control

DOI: 10.13009/EUCASS2017-317

thrusters of the Chaser. During this de-tumbling manoeuvre the robot joint torques have to be closely monitored in order to avoid violations of their limits.
Afterwards the Chaser is attached to the Target's launch adapter ring using clamps designed for withstanding the loads during the de-orbit boosts. The disposal phase foresees several boosts ending with a splash down of objects surviving the re-entry in the South Pacific Ocean. More details about e.Deorbit can be found in [4].

3. Chaser System and GNC Architecture

The Chaser is equipped with redundant navigation sensors, thrusters for attitude control and orbit control, redundant rendezvous sensors, the robotic payload and a clamping system. The attitude control thruster configuration consists of 24 thrusters. It allows commanding force and torque separately, even in case of a single thruster failure. The nominal thrust level is 22 N. The orbit control thruster package consists of 2 main engines and 4 assist engines. The main engines provide 425 N thrust, the assist engines 225 N. The main engines are used for ascent and deorbiting; the assist engines are only needed for the de-orbiting of the stack.
The navigation sensors comprise Inertial Measurement Unit (IMU), star tracker, sun sensor and GPS. The rendezvous phase requires narrow angle camera, wide-angle camera and LIDAR. The narrow angle camera is also used as inspection camera. The robotic payload consists of the robot arm, the manipulator arm camera (CAM-M) and the illumination system. The clamping system is required to rigidly attach the Chaser to the launch adapter ring of the Target. It has a trimming device allowing the alignment of the main engine thrust vector with the stack CoG. The Chaser configuration is illustrated in Figure 2. The total propellant mass required for the e.Deorbit mission is about 900 kg. Roughly 200 kg are needed for the ascent and phasing, 100 kg for rendezvous and capture, and 600 kg for the de-orbiting of the stack. Two capture attempts including collision avoidance manoeuvre and rendezvous phases are taken into account in the propellant budget.

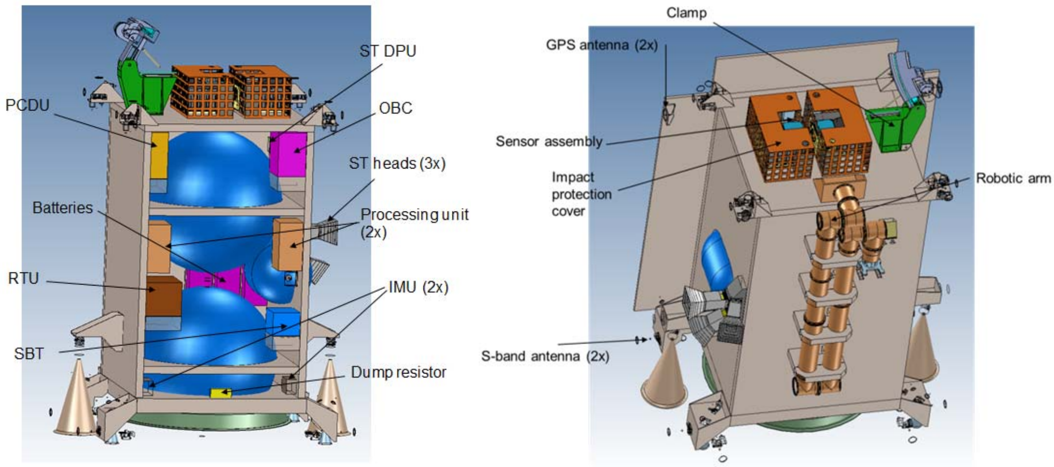

Figure 2 e.Deorbit Chaser configuration

The overall GNC system architecture is depicted in Figure 3. The GNC functions are distributed between BUS-GNC and Rendezvous GNC. The Rendezvous GNC function contains the guidance, navigation and control functions for the rendezvous phase including robot arm control. The BUS-GNC contains the standard satellite attitude and orbit control functions as needed outside the Rendezvous and Capture phase whereas the Rendezvous GNC takes over the entire satellite during Rendezvous, Capture and Stabilisation. The Fault Detection, Isolation and Recovery (FDIR) function performs health monitoring and switches to the redundant equipment, if necessary. The force and torque commands generated by the control function are translated into thruster opening commands by the thruster management function. In case of a thruster malfunction the specific thruster may be disabled by the FDIR. The thruster management function then generates the commanded forces and torques using the remaining thrusters. Furthermore safety monitoring is performed during rendezvous and capture. A collision avoidance manoeuvre (CAM) is triggered in case of safety corridor violation, independent of the health status of the Chaser. If the health monitoring detects a fault during the rendezvous phase, a CAM has to be executed before the Chaser is allowed to switch to Safe Mode. Therefore a valid collision avoidance manoeuvre sequence has to be available during the entire rendezvous phase until successful capture is confirmed. The CAM sequence depends on the current relative position,

DOI: 10.13009/EUCASS2017-317

velocity and attitude w.r.t. the Target. Therefore the Rendezvous GNC function has to calculate a valid CAM sequence in each GNC cycle.
The robot arm control function issues joint position commands in the position control mode and joint torque commands in the compliant control mode. These commands are converted to current in an inner joint motor control loop.

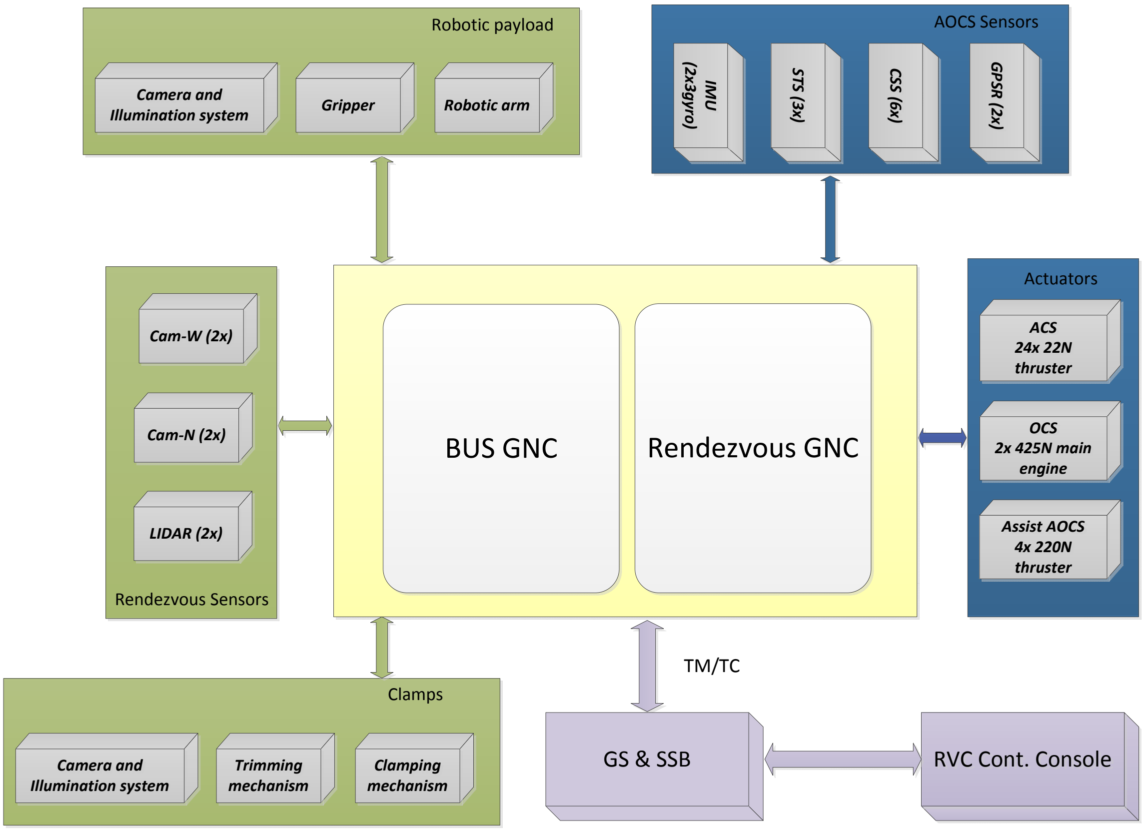

Figure 3 GNC and Avionics Architecture

4. GNC modes

The e.Deorbit mission requires various modes according to the different chaser/target configurations

- Chaser alone (ascent and phasing)
- Chaser within relative navigation distance (rendezvous, motion synchronisation and capture phase)
- Coupled by robot arm (capture, stabilisation and fixation)
- Stack (rigid connection between Chaser and Target by clamps as needed for orbit transfer and de-orbiting)

The modes for Chaser alone and Stack are similar, but not the same because of the different MCI in these phases. Especially the Stack boost control mode has to deal with large uncertainties regarding the inertia and the centre of mass. Furthermore the flexible modes of the connection between Chaser and Target with clamps and the flexible modes of Envisat's solar array have to be respected.
For the relative navigation phase it is important to note that the Chaser must not enter the Safe mode before a collision avoidance manoeuvre has been executed. The CAM can be triggered either by the Safety Monitoring or directly by the FDIR. The Safety Monitoring function is active during the relative navigation phases only and monitors the rendezvous sensors and the safety corridor during the approach. If a collision risk is detected, a CAM is commanded leading the Chaser back to the Rendezvous Entry Gate waiting ellipse, see Figure 1. The FDIR monitors the health status of the chaser platform continuously in all mission phases. If a chaser problem is detected by the FDIR during the relative navigation phase, a CAM is executed leaving the rendezvous distance and establishing a passively safe relative orbit with e/i-separation and/or drift before the chaser is switched to Safe mode. After a CAM a ground command is requested to continue the mission. Safe modes are required for the three configurations Chaser

DOI: 10.13009/EUCASS2017-317

outside relative navigation distance, coupled and stack. They rely on the same sensors and the control modes are similar, differing only by the MCI and the uncertainties.
The following attitude and position control modes are required for the e.Deorbit mission. The attitude control modes are

- Rate damping
- Slewing
- Sun pointing (battery charging)
- Local Vertical, Local Horizontal (LVLH) stabilised
- Target pointing (chaser points towards target to keep target in relative navigation sensor field of view, in combination with position control in LVLH)
- Target synchronised (chaser synchronises rotational motion with target, in combination with position control relative to target)
- Stabilisation of coupled system (de-tumbling)
- Boost control (ascent and de-orbiting)

The position control modes are

- Relative orbit acquisition (e/i-separation)
- Relative orbit station keeping (e/i-separation)
- Spiral approach (e/i-separation, homing & closing)
- Station keeping in LVLH
- Fly-around in LVLH (in combination with Target pointing attitude control for Target inspection)
- Fly-around to target's angular momentum vector in LVLH
- Approach along target's angular momentum vector in LVLH
- Position control relative to target (in combination with target synchronised attitude control mode)
- Station keeping relative to target with moving arm (in combination with target synchronised attitude control mode)
- Orbit control (boost phases, execution of ΔV command from ground)

5. Relative Navigation during Rendezvous

The vision-based navigation functions consists of a set of sensors acquiring data from different rendezvous sensors as discussed in the previous section and different algorithms processing these data on dedicated on-board hardware. These functions are:

- Line-of-sight measurement for far-range navigation based on narrow angle camera data
- Line-of-sight and range measurements for mid-range-navigation based on LIDAR data
- 6D-Pose-estimation based for close-range navigation and motion estimation based on LIDAR measurements
- Camera-based monitoring of LIDAR-based pose-estimation
- Camera-based monitoring of far- and mid-range navigation

The far-range navigation starts at the Rendezvous Entry Gate and ends at the Save Hold Point (homing). The navigation during the homing phase is based on line-of-sight measurements provided by the narrow angle camera. The navigation filter for this phase estimates the relative orbital elements from these line-of-sight measurements and uses force commands as input. Navigation filter details can be found in [2].
The closing from Save Hold Point to Parking Hold Point employs the scanning LIDAR as primary navigation sensor. Now line-of-sight and range measurements are available. The LIDAR uses a centroiding method to estimate the relative position between chaser and target. The navigation filter estimates relative position and velocity in the Local Vertical, Local Horizontal (LVLH) frame.
The LIDAR is switched to LIDAR3D mode as soon as the Parking Hold Point is reached. Now a more complex image processing on the point cloud generated by the scanning LIDAR is performed. The point cloud is matched with a geometrical model of the target. This procedure estimates relative position and attitude. The navigation filter estimates the target's attitude and angular rate in addition to relative position and velocity of the Chaser w.r.t. the Target.
The monitoring of the pose estimation is a safety critical task, especially during the proximity operations. For this task a sensor is foreseen which is independent of the primary navigation sensor. A camera-based method is proposed that uses the pose-information of the LIDAR-based approach which has to be validated. For that purpose, a wire-frame model (with hidden-line removal or silhouette extraction) of the target satellite will be projected into the most appropriate camera image for the current object distance (it can be either the wide-angle camera or even the narrow-angle camera for larger distances). Then a matching between the detected edges of the camera image and the wire-

DOI: 10.13009/EUCASS2017-317

frame model is performed. This comparison provides a consistency check or a confidence value. The image processing needed for this approach can be taken from the visual tracking function which is foreseen for the manipulation task.
If the independent monitoring measurements shall be available all the time (also during eclipse or self-shadowing), this process has to be applied to LWIR camera images.
The following block-diagram shows the main principle for the vision-based safety monitoring of the LIDAR-based pose-estimation stage.

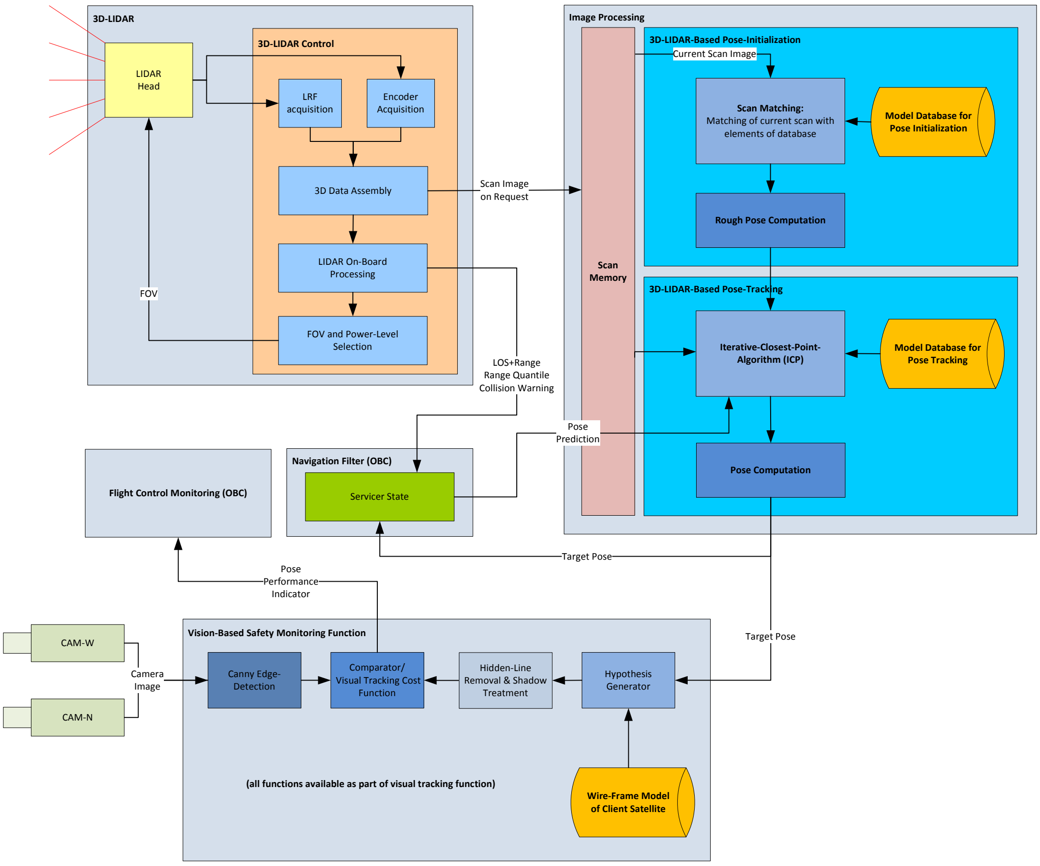

Figure 4 Principle architecture of the vision-based safety monitoring concept

Based on the pose-estimation a wire-frame model of the target satellite is projected into the camera image considering also hidden lines and shadows. The camera images are processed with a standard edge-detector and finally are compared with each other providing a pose-performance indicator or a confidence value. This approach has been analysed in preliminary tests on simulated camera sequences based on the ASTOS camera simulator.
The following simulation demonstrates the results of the proposed method for a simulated malfunction of the LIDAR-based pose-estimation. At a certain point a pose-estimation error has been introduced. The following figures depict the principal outcomes for a specific situation where the target is in front of the servicer.
All images show the projected hypothesis of the client model as a number of red dots. Beneath the red dots the costs of the distance transforms just encode the closest distance to the nearest edge in the image. Summing up these costs provides a measure for the matching quality of the LIDAR-based pose-estimation.
The following diagram demonstrates how a malfunction can be observed in the scalar confidence measure of the camera-based monitoring function.
The matching quality shows a significant increase in the cost function. Until t = 8217 s the LIDAR-based pose-estimation works well and provides the correct pose. At t = 8217 s a flipping of the roll-angle by 180° has been simulated in order to test a situation where the pose-estimation provides a wrong measurement. Similar results can be obtained if the pose-estimation freezes. Then the increase of the matching quality error is not so instantaneous but increases more slowly. In any case the matching quality error exceeds a certain threshold indicating a malfunction.

DOI: 10.13009/EUCASS2017-317

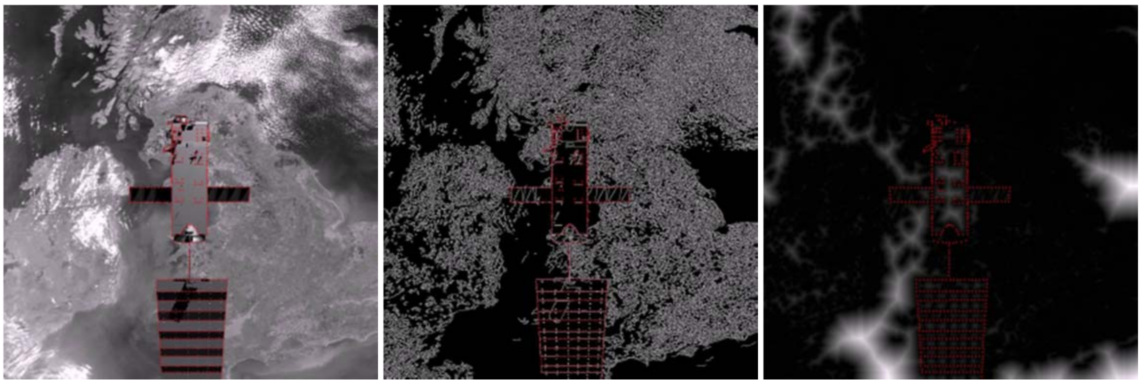

(a) (b) (c)

Figure 5 (a) simulated camera image coming out of the ASTOS simulator. (b) Result of edge extraction using a Canny edge detector. (c) Result of distance transform used for cost computation.

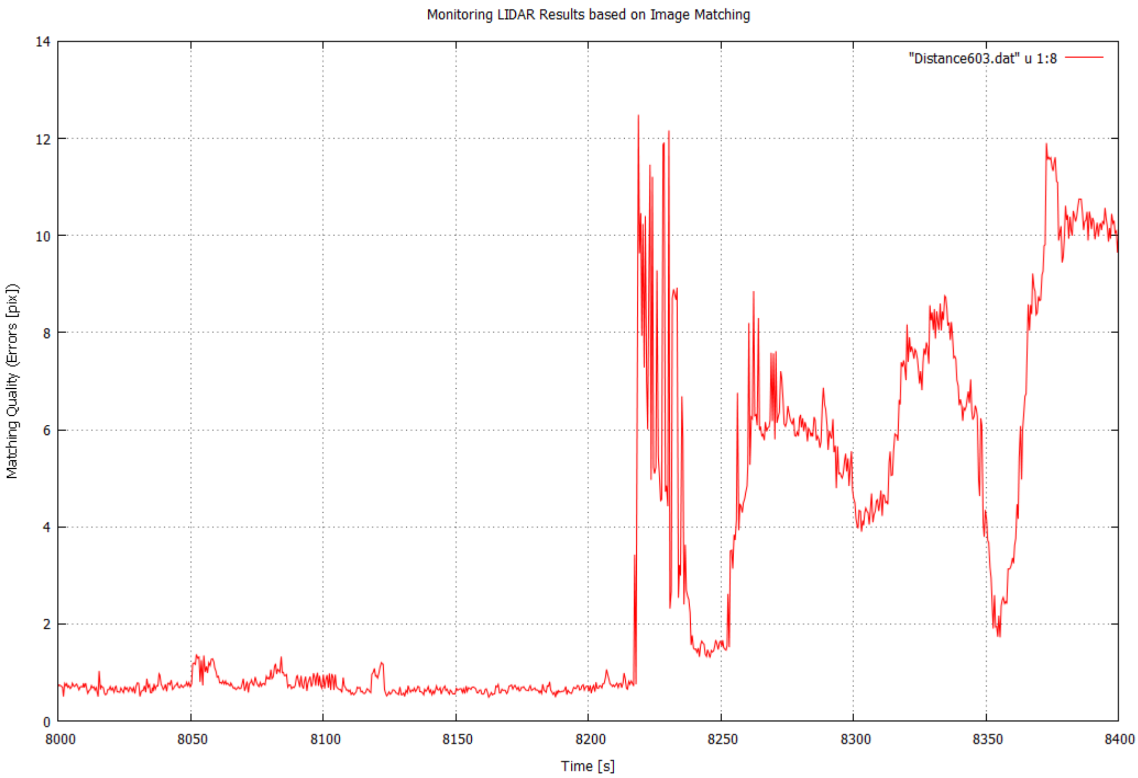

Figure 6 Matching quality vs. time: The LIDAR error occurred at t = 8217 s.

6. Coupled Control

The chaser has to perform station keeping at the Capture Point during the grasping operations performed by the robot arm. The force and torque commands can be split into three contributions:

- Feed forward term stemming from robot control
- Feed forward term stemming from guidance
- Feedback term from control

The feed forward term from robot control provides the forces and torques generated in the arm base by the robot to the chaser GNC. The guidance commands the forces and torques required for compensating the centrifugal forces due to the tracking of the desired position and attitude relative to the tumbling target. The feedback term

DOI: 10.13009/EUCASS2017-317

compensates all control errors including navigation errors, thruster and chaser MCI uncertainties, and disturbances due to propellant sloshing.
A PD controller tuning and a robust control design (μ-synthesis) has been performed taking into account the sloshing effects and the other aforementioned uncertainties. The PD controller bandwidth is 0.2 rad/s for position control and 0.3 rad/s for attitude control. It works well for a rigid body system, but is instable for the large sloshing masses without baffles. Even with μ-synthesis a robustly stable control design could not be achieved for the plant without baffles due to the large sloshing masses and their uncertainties. Therefore baffles are foreseen in the design. The baffles reduce the sloshing masses by one order of magnitude and increase the damping by more than one order of magnitude. The sloshing frequency is significantly suppressed by the robust controller, but even the PD controller is robustly stable for the modelled uncertainties for the case with baffles.
The aim of the robot arm control is to minimize the error between the current end-effector pose and the desired pose at the grasping point, or otherwise, to follow a reference trajectory. For the e.Deorbit scenario, the grasping point is located at the Target's launch adapter ring.
Usually, a torque controller is preferred in case of a possible interaction with the Target. Indeed the robot might push the Target away if the robot controller does not have impedance behaviour with the Target. Therefore, the desired performance of the torque controller will be specified through Cartesian impedance, namely a definition of mass-spring-damper parameters for each Cartesian direction in the robot end-effector frame [6].
The coupled-controller consists of two separate control elements, one being the Chaser controller (GNC) and the other being the robot controller. The GNC operates relative to the Target in order to control the attitude of the Chaser with a sampling frequency of 1 Hz. The robot controller has a higher bandwidth and its sampling time is 1 ms (1 kHz frequency). Both controllers must be coupled through a designed interface, see Figure 7. The Chaser provides the relative pose (position and orientation) between Chaser and Target to the robot controller, and the robot controller exchanges data with the Chaser by means of forces and torques computed at the base of the robot. More details about the coupled control of chaser and robot arm can be found in [5].

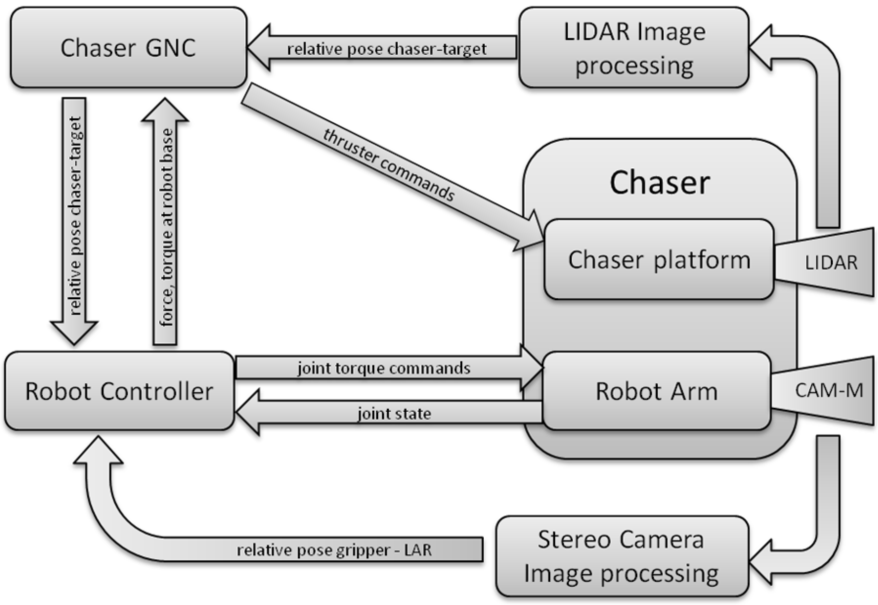

Figure 7 Data exchange between sensors, actuators, robot controller and Chaser GNC

7. Capture process

The detailed capture process is summarised in Table 1. At the Parking Hold Point the arm is unfolded from its initial position at launch. The arm follows a pre-planned trajectory until the desired joint angles are reached. The approach and motion synchronisation from Parking Hold Point until Capture Point are performed in this configuration. At the Capture Point the gripper is positioned at about 1 m distance to the Grasping Point at the target's launch adapter ring. The arm follows a pre-planned trajectory in joint space again. The visual servoing system is enabled to initialise and track the POSE between gripper and Grasping Point. This POSE information is needed to position the gripper with open capture jaws at the Grasping Point.

DOI: 10.13009/EUCASS2017-317

The gripper jaws are closed as soon as the gripper sensors confirm that the gripper position and orientation is reached for capture. The first closure establishes a soft connection between gripper and Grasping Point ensuring, that the launch adapter ring can no longer escape. This first closure is quick (<0.5 s), but not yet rigid. The forces and torques have to be limited. Therefore the joints are not actuated during the rigidisation of the gripper and the joint brakes are not engaged. The arm can basically move freely, but provides significant damping due to the friction in the joints, especially in the gear box. The backdrive torque in the joints is limited to 40 Nm. The rigidisation of the gripper is performed in the next step. The duration of the gripper rigid closure is about 15 s. Now a rigid connection between gripper and Grasping Point is established.
As soon as the rigid gripper closure is confirmed, the arm is rigidised. The arm is operated in active compliance mode for this purpose. The joint brakes are engaged as soon as joint rates are below a threshold and the Chaser is at the desired relative position and orientation at the Capture Point. Now the de-tumbling of the coupled system begins. As soon as the angular rate is below a threshold, the fixation of the chaser at the target's launch adapter ring using the clamps can begin. The procedure is quite similar to the detailed capture process. The arm positions the chaser relatively to the clamping point at the launch adapter ring, such that the clamp sensor system can perform the POSE estimation. Next the clamps are positioned at the launch adapter ring and closed (stack configuration). After confirmation of successful clamping the thrust vector of the Chaser's main engines are aligned with the stack CoG. Now the stack can be re-oriented for battery charging, waiting for the de-orbiting and disposal window and then for the corresponding boosts.

Table 1 Detailed capture process

Phase	Description	Robot arm control mode	Chaser control mode
Unfold arm	Arm is unfolded from launch folded position	Control of pre-planned trajectory	station keeping at Parking Hold Point
Gripper positioning for grasping point identification	The gripper is positioned at about 1 m distance to the grasping point allowing POSE estimation of the grasping point (5 dof) by the Laser pattern projectors and gripper vision system camera.	Control of pre-planned trajectory	Station keeping at Capture Point
Gripper positioning for grasping	The gripper is positioned at the grasping point with open capture jaws based on visual tracking	Active compliant (DLR) Position control (MDA)	Station keeping at Capture Point
Gripper form closure	Gripper establishes soft connection with grasping point (LAR can no longer escape)	Active compliant	Station keeping at Capture Point
Gripper rigid closure	Gripper establishes rigid connection with grasping point. During this phase the joints are not actively actuated. The backdrive torque in the joints allows final alignment of the gripper.	Backdrive passive compliant, joint brakes not engaged	Station keeping at Capture Point
Arm rigidisation	Rigidisation of joints by active compliant control until joint brakes can be engaged	Active compliant	No control
De-tumbling	Coupled system is de-tumbled	Passive compliant, brakes engaged	De-tumbling
Fixation	Chaser is attached to target launch adapter ring using clamps	Active compliant	No control

8. GNC Performance

Extensive Monte Carlo (MC) simulations have been performed to demonstrate that the system design is compliant with the performance requirements listed in Table 2. 100 runs have been performed, leading to 63% confidence level for 99% probability of success, i.e. one simulation run out of 100 with violations of requirements would be accepted. Accepting 3 runs with violations would raise the confidence level to 95%. Furthermore the simulation results give insight to the driving parameters for the propellant consumption. Figure 8 and Figure 9 show exemplary results for the closing and the motion synchronisation phase. The GNC performance requirements are met. No violations of the requirements occurred in the simulations. The position error is about two orders of magnitude lower during the motion synchronisation phase than in the preceding rendezvous phases. During homing and closing the GNC

DOI: 10.13009/EUCASS2017-317

performance requirements are quite relaxed in comparison to the requirements for the motion synchronisation and capture. The reasons are the save distance and the passively safe approach trajectory design.
The proximity operations have to be performed in force motion control mode. The comparison of Figure 10 and Figure 11 shows clearly the expected increase in propellant consumption per time when the chaser is operated in forced motion control mode. Figure 11 shows an additional increase of the slope in the propellant consumption at about 650 s. This is the point in time where the chaser synchronises its motion fully with the target. The consumption is rather moderate as long as the chaser is controlled in the LVLH frame. As soon as the chaser has to follow the tumbling motion of the target, it has to compensate the centrifugal forces, which leads to the high consumption. Therefore the duration during which the chaser is in the motion synchronisation mode is a driver for the total propellant consumption in the rendezvous and capture phase. Furthermore the consumption is driven by the angular rate of the target; it scales with the square of the angular rate. The design case in e.Deorbit Phase B1 was 5°/s. Today this value seems to be very conservative.

Table 2 GNC Performance Requirements

Phase	**Position [m]**	**Velocity [m/s]**	**Attitude [deg]**	**Angular rate [deg/s]**
Safe Mode	-	-	5	0.5
Ascent and phasing	100	1 -	1 during boost 5 during drift periods	0.1 0.5
Rendezvous, Homing	10% of ROE	-	5	0.5
Rendezvous, Closing	10	0.1	5	0.5
Rendezvous, Sync. & Capture	0.05	0.01	2	0.5
Stabilisation	-	-	-	0.5
De-orbiting	-	0.3 -	1 during boost 5 during drift periods	0.1 0.5

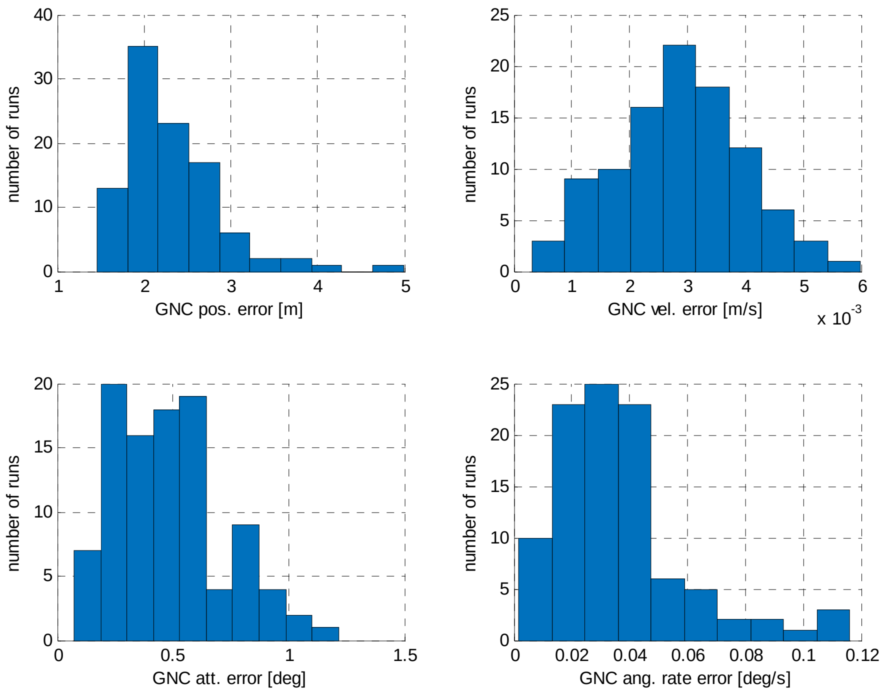

Figure 8 MC result for closing, final GNC performance

DOI: 10.13009/EUCASS2017-317

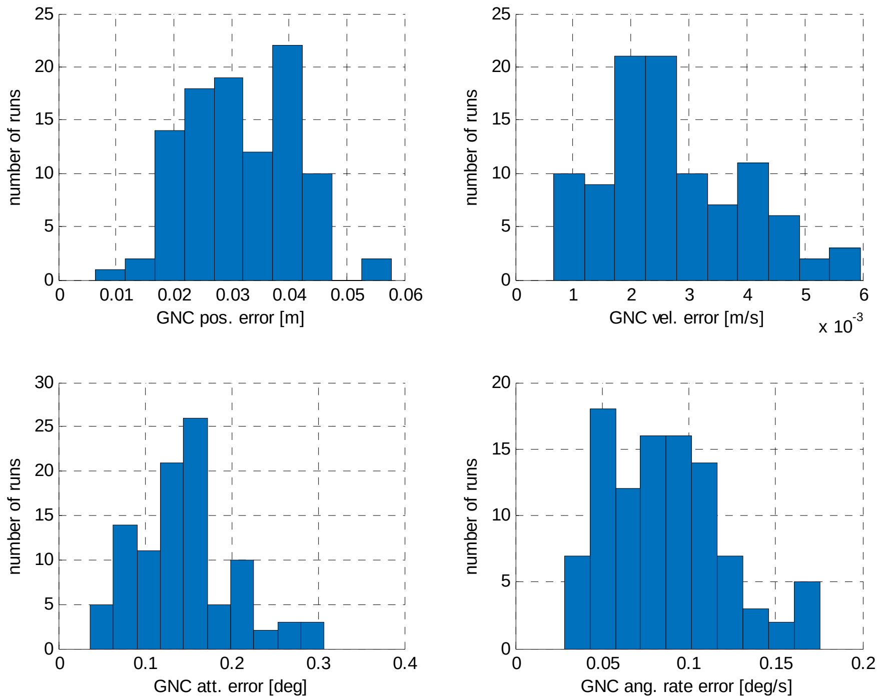

Figure 9 MC result for motion synchronisation, final GNC performance

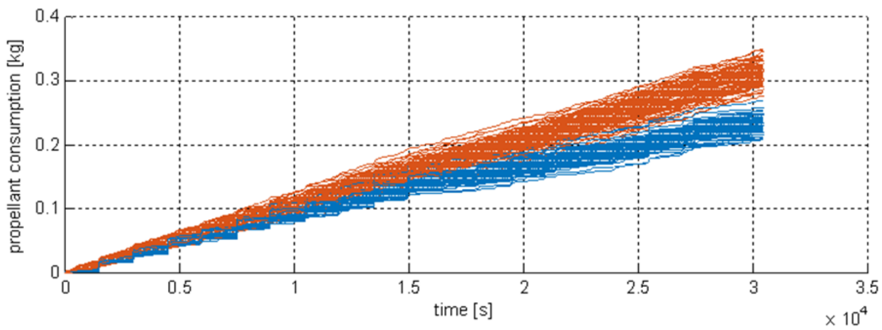

Figure 10 MC result for closing, propellant consumption for position control (blue) and attitude control (red)

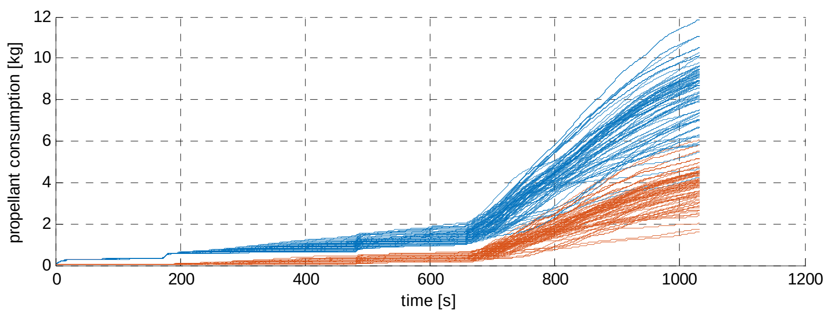

Figure 11 MC result for motion synchronisation, propellant consumption for position control (blue) and attitude control (red)

DOI: 10.13009/EUCASS2017-317

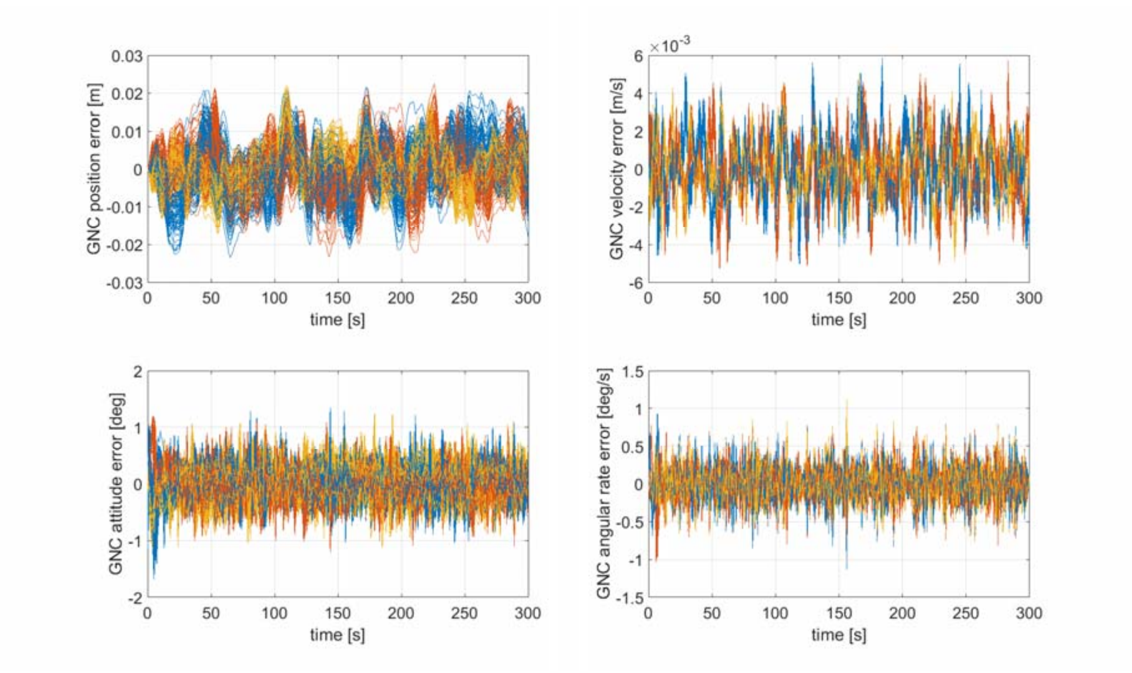

Figure 12 MC results, GNC performance during capture operations, Target angular rate 5°/s around random axis, limited to 30° w.r.t. Target y/z plane (close to flat spin)

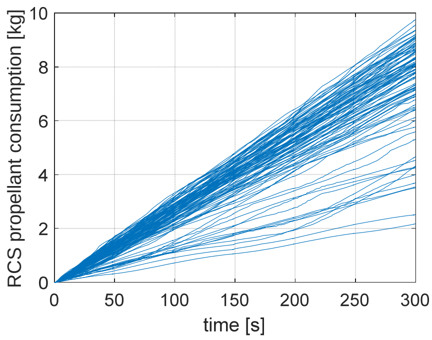

Figure 13 MC results, Propellant consumption during capture operations, Target angular rate 5°/s around random axis, limited to 30° w.r.t. Target y/z plane (close to flat spin)

The gripper positioning error and the orientation error are plotted in Figure 14. During the first 30 seconds, the designed robot control moves the end-effector from the starting position to the grasping point and it keeps the track of it for all the simulation time. The limited residual error is due to the slow update of the data exchanged by the Chaser control with the Robot control, i.e. 1 Hz and 1000 Hz sampling frequency, respectively. Note that the detection error, which comes from the pose estimation algorithm (gripper to grasping point relative navigation), has not been taken into account in this simulation. Therefore the gripper positioning and orientation error are underestimated. Currently no consolidated performance model of the gripper camera and illumination system is available.

The Chaser GNC is active during the entire simulation. The impact of the Chaser thruster firing at 1 Hz is barely visible in the plots. More obvious is the very low frequency vibration of the gripper position and attitude which is linked to the tumbling motion of the target.

DOI: 10.13009/EUCASS2017-317

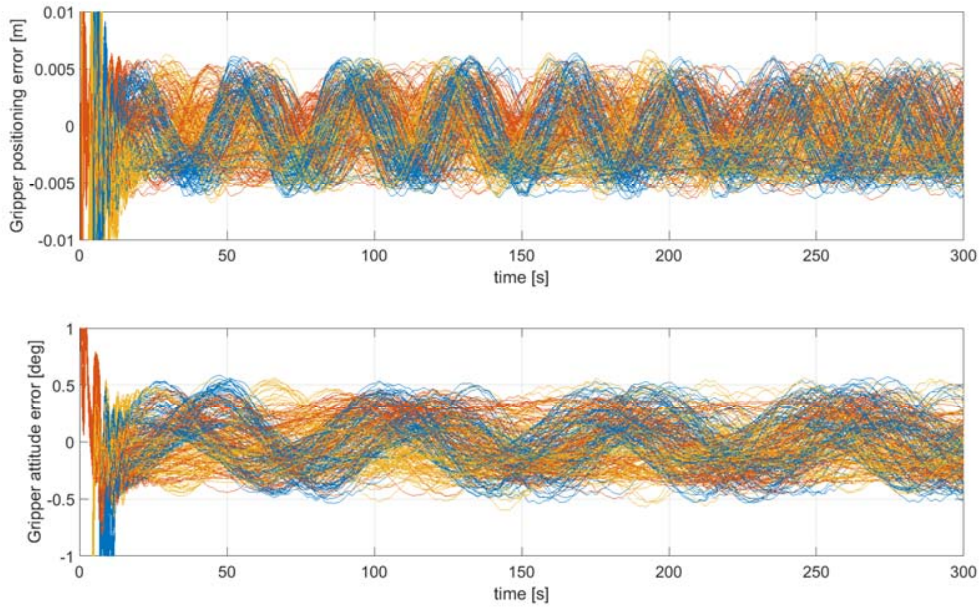

Figure 14 MC results, Gripper positioning and attitude errors, Target angular rate 5°/s around random axis, limited to 30° w.r.t. Target y/z plane (close to flat spin)

9. Target Stabilisation and De-orbiting

After successful capture and rigidisation of the robot arm, the chaser has to stabilise the coupled system. The challenge here is the limited joint torque capacity of the robot arm. The coupled system is considered as stabilised as soon as the angular rate drops below 0.5°/s. The de-tumbling function predicts the joint torques and reduces the commanded torques accordingly, if a violation of the joint torque limit is predicted.

The propellant consumption and the maximal occurring joint torques for the target stabilisation depend strongly on the initial angular rate of the target. The Monte Carlo simulation results in Figure 15 and Figure 16 show that the joint torques remain below the limit imposed by the free tumbling motion of the coupled system after capture. The maximal torques are about 150 Nm in the joints 4 and 7 for the given initial target tumbling rate of 5°/s.

After stabilisation the chaser is connected to the target using clamps. This connection is much stiffer than the robot arm and allows performing the deorbit boosts. The clamping mechanism has a trimming capability to ensure that the thrust vector of the main engines is aligned with the stack CoG. During this fixation phase GNC thruster firings are inhibited.

The de-orbiting manoeuvre is split into three manoeuvres. Two manoeuvres are reducing the perigee altitude, the third manoeuvre is the final de-orbit boost. The perigee altitude after the second boost is limited by the controllability of the stack in relatively dense atmosphere. It must not be lower than 200 km. The boosts are performed by the main engines and by the assist engines. The assist engines are operated in off-modulation. They support the boost and perform the attitude control for the transversal axes.

DOI: 10.13009/EUCASS2017-317

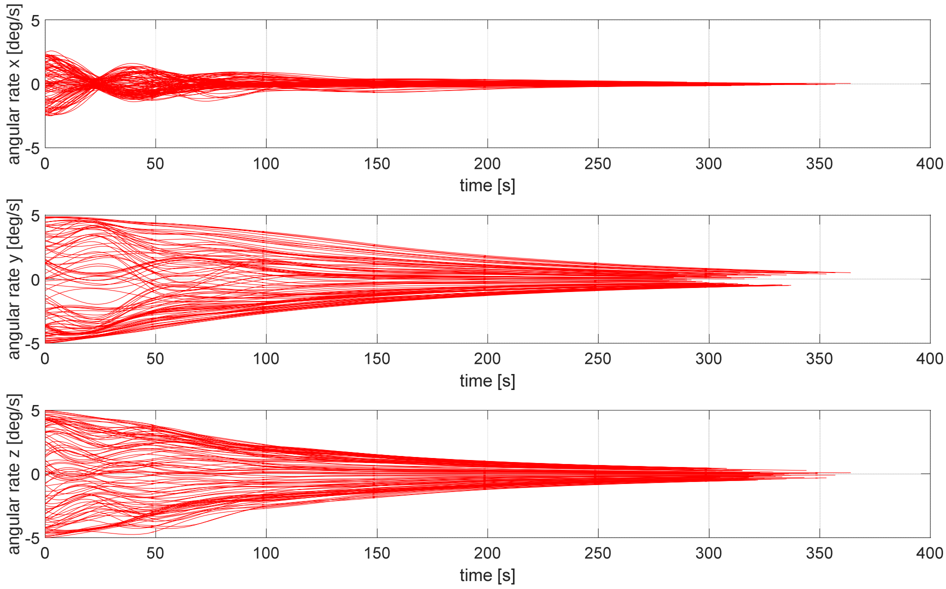

Figure 15 Angular rates during stabilisation, Monte Carlo Simulation, 100 runs, initial spin axis orientation: random angle 0-30° between spin axis and body YsZs plane, spin rate 5°/s

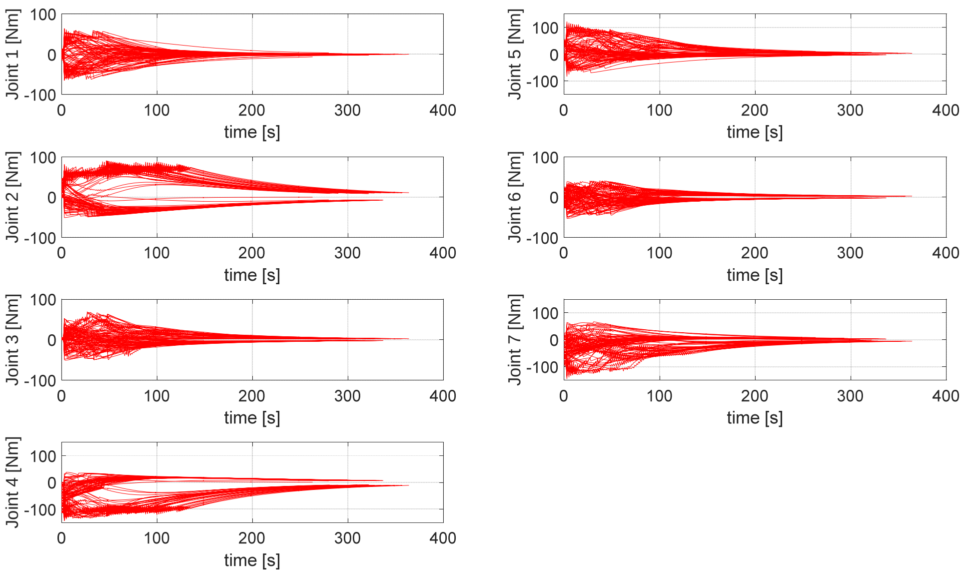

Figure 16 Joint torques during stabilisation, Monte Carlo Simulation, 100 runs, initial spin axis orientation: random angle 0-30° between spin axis and body YsZs plane, spin rate 5°/s

DOI: 10.13009/EUCASS2017-317

10. Summary and Conclusions

The GNC system architecture for the space debris removal mission e.Deorbit is presented. It comprises a sensor suite allowing absolute and relative navigation. The chaser is equipped with a redundant sensor system. The actuators comprise main engines and assist engines for the ascent and de-orbiting boosts. The attitude control between the boosts and the rendezvous manoeuvres are performed by a thruster system. Due to the short mission duration no reaction wheels are needed. The GNC functions are split between BUS GNC and rendezvous GNC. The BUS GNC contains the standard satellite AOCS functions, whereas the additional GNC functions required for the rendezvous and capture are covered by the rendezvous GNC.
The proximity and capture operations are the most critical mission phases. The primary navigation sensor for this phase is a scanning LIDAR. The processing of the LIDAR data allows the full pose estimation, i.e. the estimation of relative position and attitude between Chaser and Target. The safety monitoring is performed by an independent sensor. Camera images are compared with expected images based on the pose estimation. If the matching error exceeds a given threshold, a fault is detected.
The coupled control performance of chaser platform and robotic arm during capture operation drives the required opening width of the gripper. The interfaces between the two separate controllers are defined and a control design has been performed taking into account the driving uncertainties.
The propellant consumption during rendezvous and capture is mainly driven by the duration of the synchronised motion phase. During this phase the chaser tracks the tumbling motion of the target and has to compensate the centrifugal forces due to the tumbling of the target. Therefore the duration of the capture operations is limited to 5 minutes.
After successful capture the compound of chaser and target has to be stabilised. During this de-tumbling manoeuver the torques occurring in the joints have to be closely monitored. The de-tumbling strategy applied here reduces the commanded torques as far as necessary, if the predicted joint torques are higher than their limit.
The de-orbiting manoeuvre can be performed after fixation of the chaser with its dedicated clamps on the launch adapter ring of the target. The clamps have a trimming capability to align the stack CoG with the thrust vector of the main engines. The de-orbiting manoeuvre is split into three boosts. The first two boosts lower the perigee to 200 km, the third boost is the final de-orbiting burn. The main advantage of this de-orbiting strategy is that requires less propellant than a strategy with a lower number of boosts, because the boosts are performed closer to the apogee. Furthermore the second and third boost can compensate boost errors of the preceding boost leading to more precision when targeting at a designated area in the South Pacific Ocean.

Acknowledgement: The e.Deorbit Phase B1 contract was carried out under a program of and funded by the European Space Agency.

References

[1] "Space Debris: The ESA Approach", 7th European Conference on Space Debris, Darmstadt, Germany, 2017
[2] Telaar, J., Schlaile, C., and Sommer, J. 2015. Guidance and Navigation for Rendezvous with an Uncooperative Target. 6th European Conference for Aeronautics and Space Sciences (EUCASS), St. Petersburg, Russia
[3] D'Amico, S. 2010. Autonomous Formation Flying in Low Earth Orbit. PhD thesis. Technical University of Delft. ISBN 978-90-5335-253-3.
[4] Estable, S., Telaar, J., et al. 2017. Definition of an Automated Vehicle with Autonomous Fail-Safe Reaction Behavior to Capture and Deorbit Envisat, 7th European Conference on Space Debris, Darmstadt, Germany
[5] Telaar, J., Estable, S., et al. 2017. Coupled Control of Chaser Platform and Robot Arm for the e.Deorbit Mission, 10th International ESA Conference on Guidance, Navigation & Control Systems, Salzburg, Austria
[6] Siciliano, et al, “Robotics: Modelling, planning and control”, Springer, 2009.